Period Doubling Bifurcations & Nonlinearities in Semiconductor-Gas Discharges

ILKER U. UZUN-KAYMAK

Department of Physics,

Middle East Technical University,

06800, Ankara, TURKEY

27 July 2020

NSTX-U Magnetics Meeting

METU-ODTÜ

What is the motivation for studying nonlinear structures?

- **Nonlinear pattern formations are ubiquitous in nature.**
  - In biology: Nerve pulses, cell structures.
  - In physics: Patterns in cosmology, current filament formations in gas discharges.

- **A DC driven Semiconductor-Gas Discharge (SGD) system is designed to study nonlinearity and period doubling features.**

- **Current filament formations can be due to different mechanisms.**
  - Space charge induced electric field redistribution,
  - Thermal effects.
    - Reference: Yu. P. Raizer, M.S. Mokrov, Physics of Plasmas, 20, 101604(2013).

DC barrier discharge systems are compelling.

- Unlike Dielectric Barrier Discharges (DBDs) SGDs can be operated via a DC field.
- The reactive nature of the barrier can be described using an external circuit equation.

$$C_s R_s \frac{dU(t)}{dt} = V_{DC} - U(t) - R_s I(t)$$

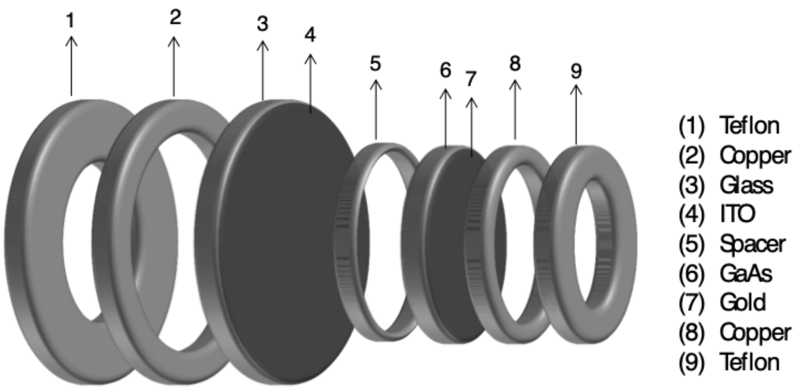

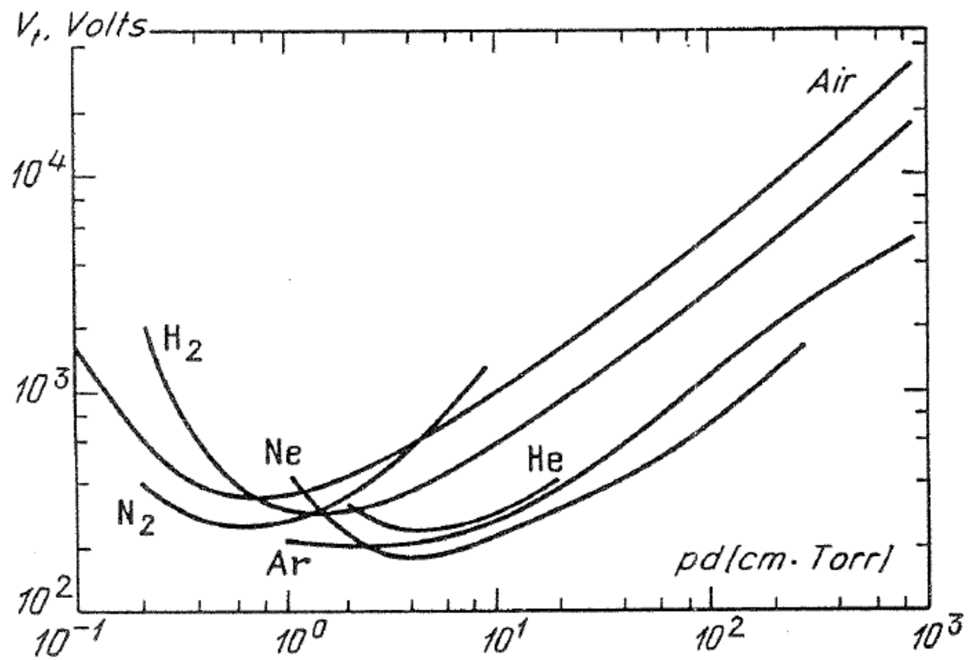

Figure courtesy: Gas Discharge Physics by Y. P. Raizer, p.134, Springer-Verlag.

Glow discharge can be modeled using fluid equations.

- DBDs and SGDs are often treated as drift-diffusion systems.
- Previous 2D simulations show Hopf type and Turing-Hopf type bifurcations.
- Ionization impact length: α_0
- Number density: $n_{e,i}$
- Mobility: $\mu_{e,i}$
- Particle flux: $\Gamma_{e,i}$
- Diffusion term: $D_{e,i}$
- Electric field: E
- Electrostatic potential: Φ
- Electrostatic approximation is used.

$$\partial_t n_e + \nabla . \boldsymbol{\Gamma_e} = |n_e \mu_e E| \alpha_0 e^{-E_0/|E|}$$

$$\boldsymbol{\Gamma_e} = -n_e \mu_e \boldsymbol{E} - \mathcal{D}_e \nabla n_e$$

$$\partial_t n_i + \nabla . \boldsymbol{\Gamma_i} = |n_e \mu_e E| \alpha_0 e^{-E_0/|E|}$$

$$\boldsymbol{\Gamma_i} = n_i \mu_i \boldsymbol{E} - \mathcal{D}_i \nabla n_i$$

$$\nabla . \boldsymbol{E} = \frac{e}{\varepsilon_0}(n_i - n_e) \; ; \; \boldsymbol{E} = -\nabla \phi$$

$$\nabla^2 \phi = -\frac{e}{\varepsilon_0}(n_i - n_e)$$

Numerical simulations are developed scanning the parameter space.

- **Numerical simulations are based on the experimental parameters:**
  - N_2 gas at $p \approx 30 - 40 mbar$,
  - Discharge gap thickness $d_{gap} = L = 1mm - 1.4mm$,
  - $d_s = 350 \mu m$ (GaAs:Cr in particular),
  - $V_{\text{app}} \approx 580V - 1kV$,
  - Conductivity $\approx 10^{-8} / \Omega \cdot cm$.

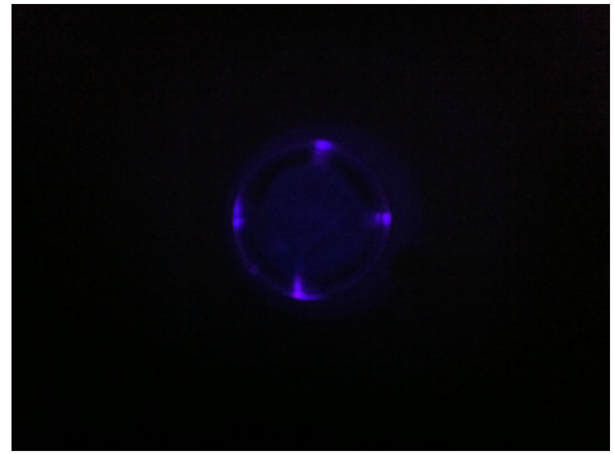

- **Discharge can vary depending on the semiconductor starting from Townsend dark to normal glow discharge.**
  - Observed current values are on the order of $10^{-4} - 10^{-3} A$.
  - Corona discharge can be observed at higher voltage/lower gas pressure settings .

Numerical simulations are conducted using COMSOL® Multiphysics software.

- Start with the continuity equation for the charged particle species

$$\partial_t n_{e,i} + \nabla \cdot \Gamma_{e,i} = S$$

- Particle flux terms are:

$$\Gamma_e = -n_e \mu_e E - D_e \nabla n_e$$
$$\Gamma_i = n_i \mu_i E - D_i \nabla n_i$$

- The source term $S = |\Gamma_e| \alpha = |\Gamma_e| Ape^{-Bp/|E|}$ is defined using the classical Townsend approximation where A, B are constants and p is the pressure.

- Types of ionization to consider
  - The α-process of electron impact ionization,
  - The γ-process of electron emission by ion impact on the cathode.

The physical system can be described in COMSOL®.

- **At the anode ($x = 0$):** $n_i = 0$; $\Gamma_e = 0$; $\Phi = 0$
- **At the cathode ($x = L$):** $\Phi = -U$ **;**

$$J_g = e(\Gamma_i - \Gamma_e) + \epsilon_0 \frac{\partial E}{\partial t}; \text{ where}$$

$$|\Gamma_e| = \gamma |\Gamma_i|$$

- **The problem is 1D as long as $R \gg L$ where L is the discharge gap, and R is the radius of the electrode.**

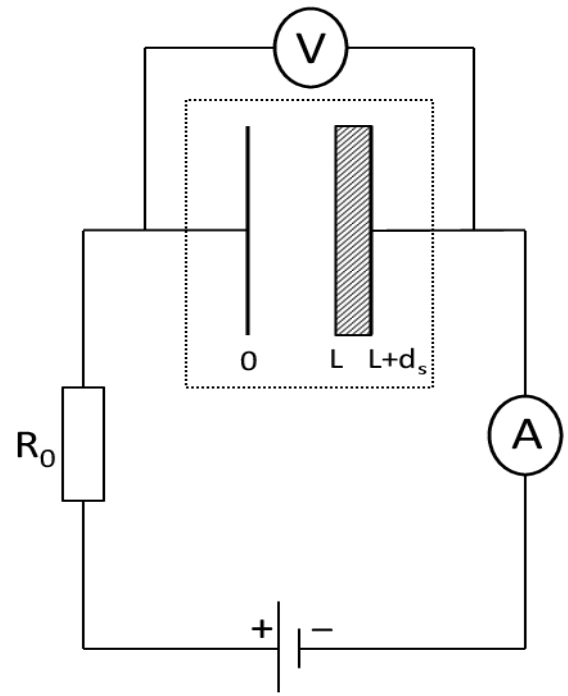

d_s is the thickness of the semiconductor.

The set of equations are solved for 1D geometry using the Comsol Multiphysics® software.

- To match the experiment

$$\epsilon_s = 13.1$$

$$\mu_i p = 1140 \text{ cm}^2\text{Torr/(Vs)}$$

$$\mu_e p = 4.4 \times 10^5 \text{ cm}^2\text{Torr/(Vs)}$$

$$\gamma = 0.08$$

- $$A = 12 \text{ (Torr.cm)}^{-1}$$

$$B = 342 \text{ V(K.cm)}^{-1}$$

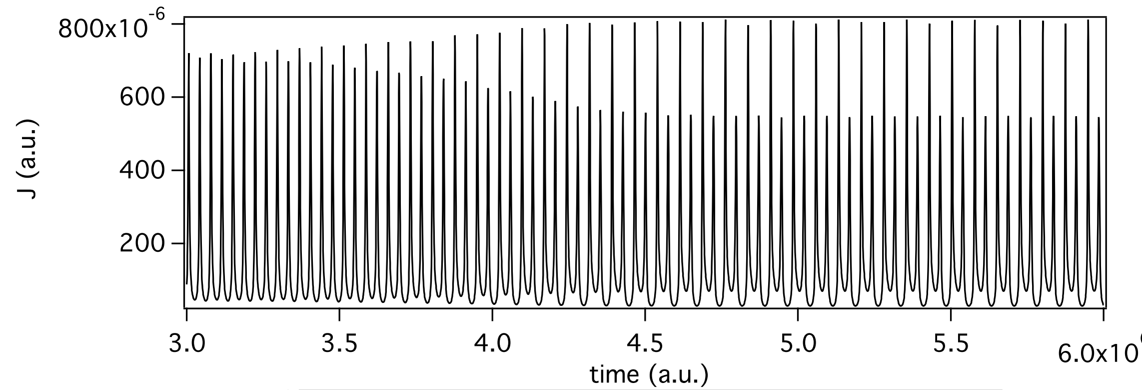

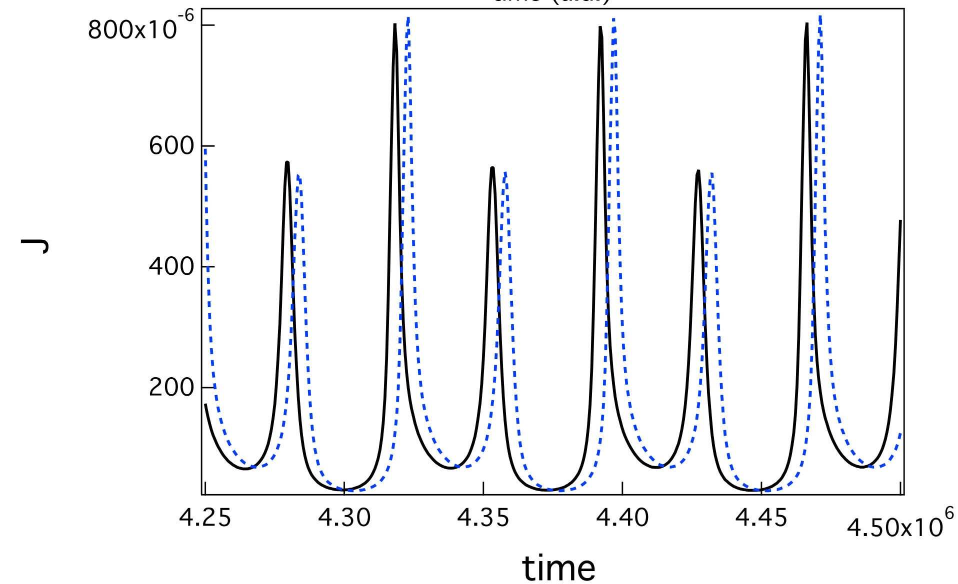

The current characteristics. Solid line is for drift only, whereas the dashed line is for particle drift and diffusion combined.

DC Barrier discharge: Experimental setup

- Nitrogen gas at sub-atmospheric pressures.
- 30 mbar ~ 23 Torr
- Any semiconductor can be used as a cathode.
- ITO coated glass as anode.
- Planar electrodes: can be as large as 2” in diameter.
- Electrode separation ~ 1mm separation.
- Parameter scan 500 V- 1.2 kV.

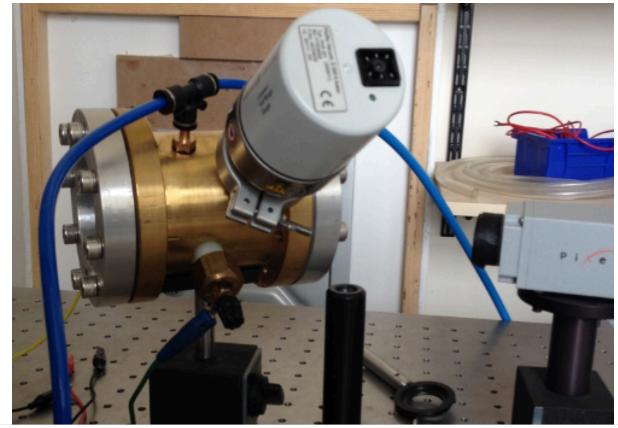

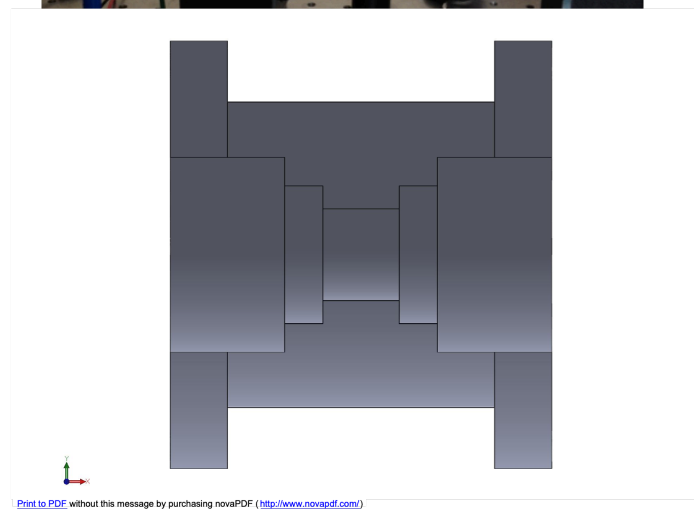

Current and voltage fluctuations are measured.

- Voltage fluctuations across the system is measured using a voltage divider circuit.
- Current fluctuations are measured using an additional ballast resistor R_0.
- Fluctuation measurements are acquired using a fast oscilloscope Lecroy 6100. Data is sampled at a 1MS/s sampling rate .
- Usual record length is about 4s long.

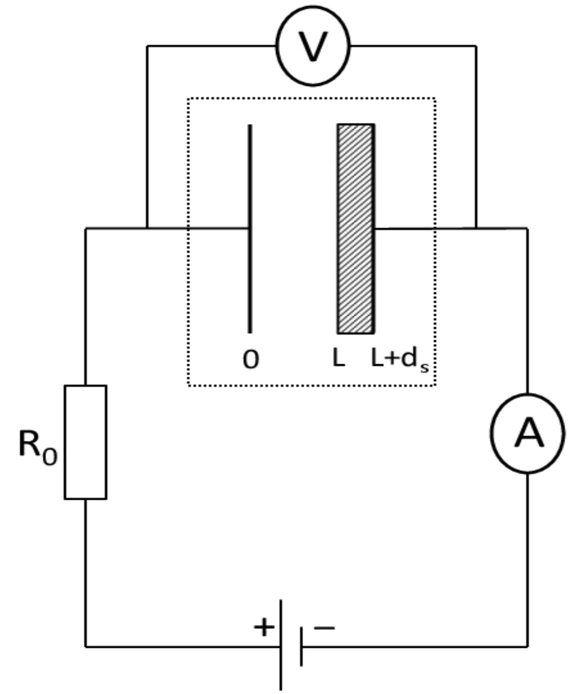

L : plasma gap thickness
d_s: semiconductor thickness

Experimental data are compared with the simulation data.

- **For a given set of parameters, experimental data and the numerical simulations of fluctuations oscillate at the same frequency.**
- **Current fluctuation amplitudes are higher in numerical simulations.**

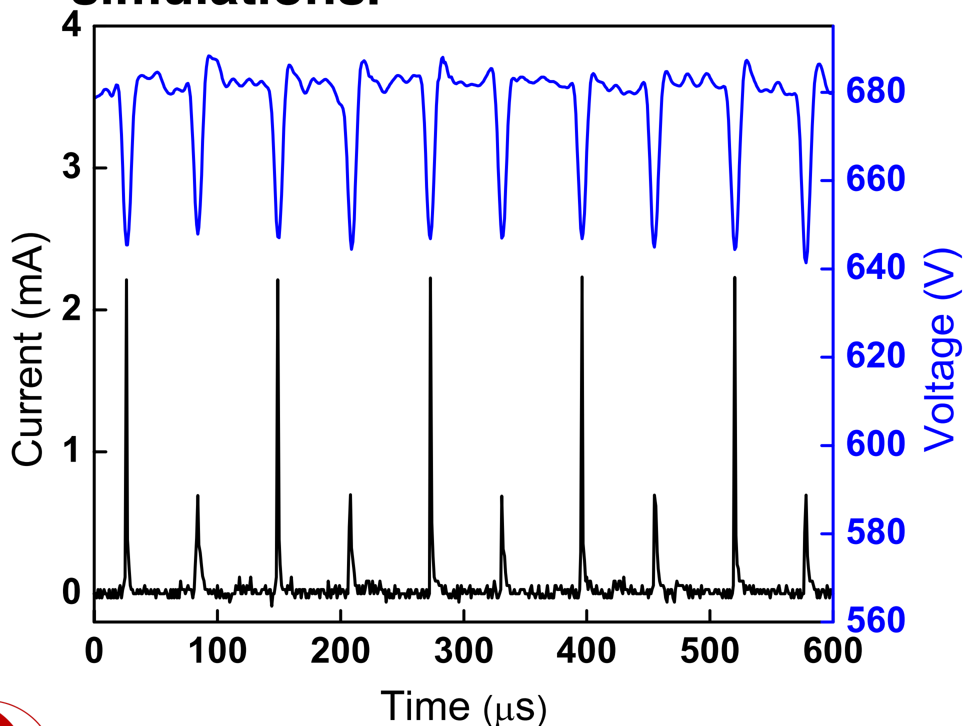

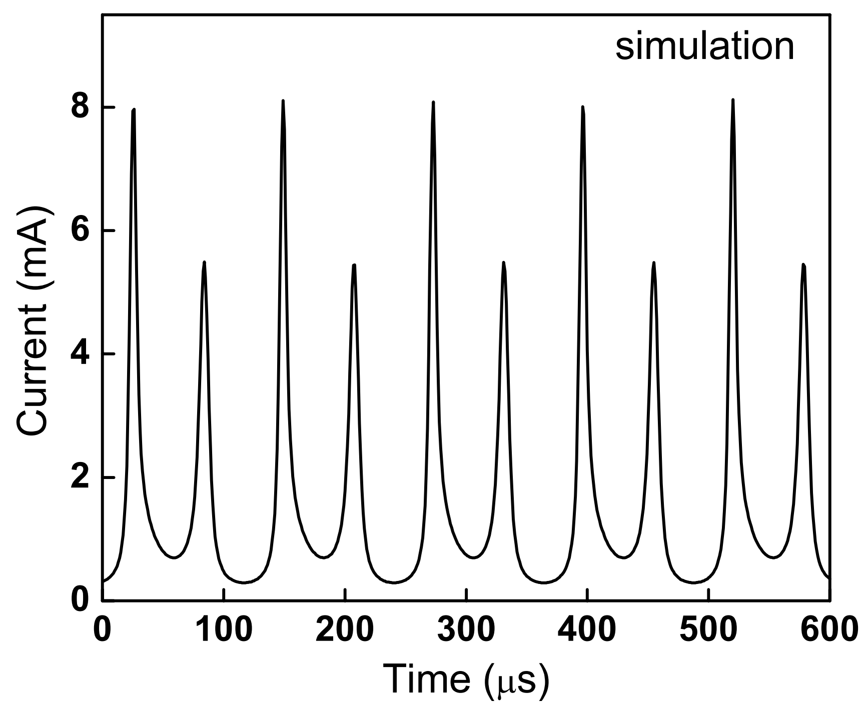

Fluctuation data are oscillatory.

- **At low applied voltage the oscillations are spatially homogenous and single frequency.**
- **As the applied voltage increased, frequency shifts towards higher values.**
- $V_a < V_b < V_c$

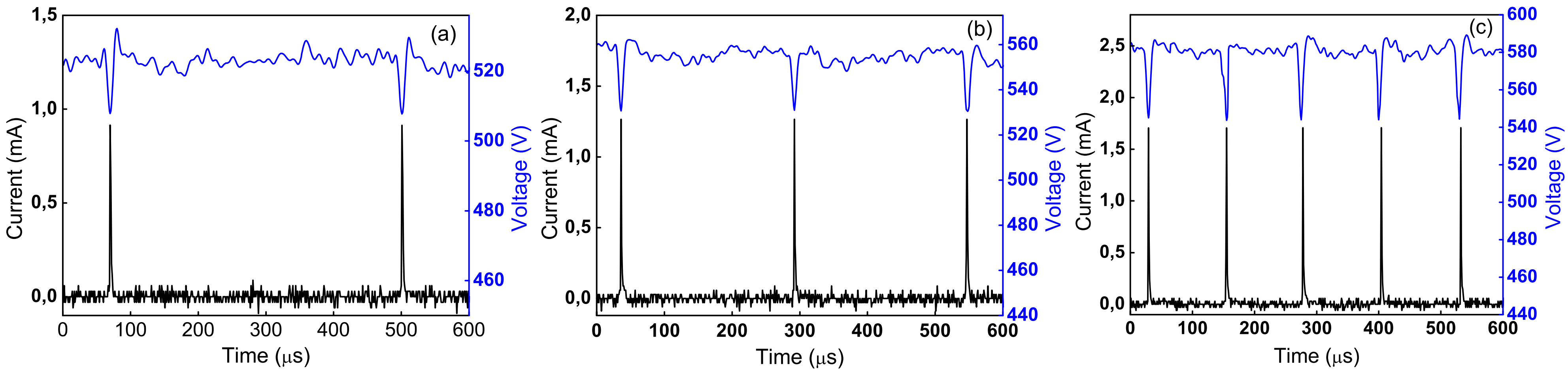

– D. Mansuroglu, I.U. Uzun-Kaymak, 2017 Plasma Sci. Technol. 19, 015401

Is this “period doubling”?

- **As the applied voltage is increased, subharmonics appear in order: f_0, $f_0/2$, $f_0/4$ where f_0 is the fundamental frequency.**
  $V_d < V_e < V_f$

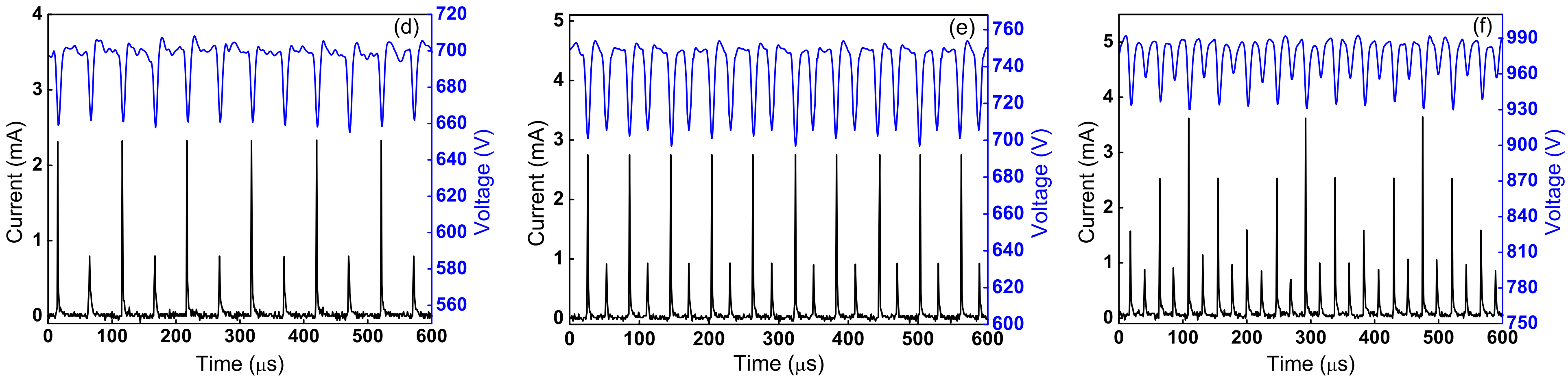

  – D. Mansuroglu, I.U. Uzun-Kaymak, 2017 Plasma Sci. Technol. 19, 015401

How are these I-V fluctuations linked?

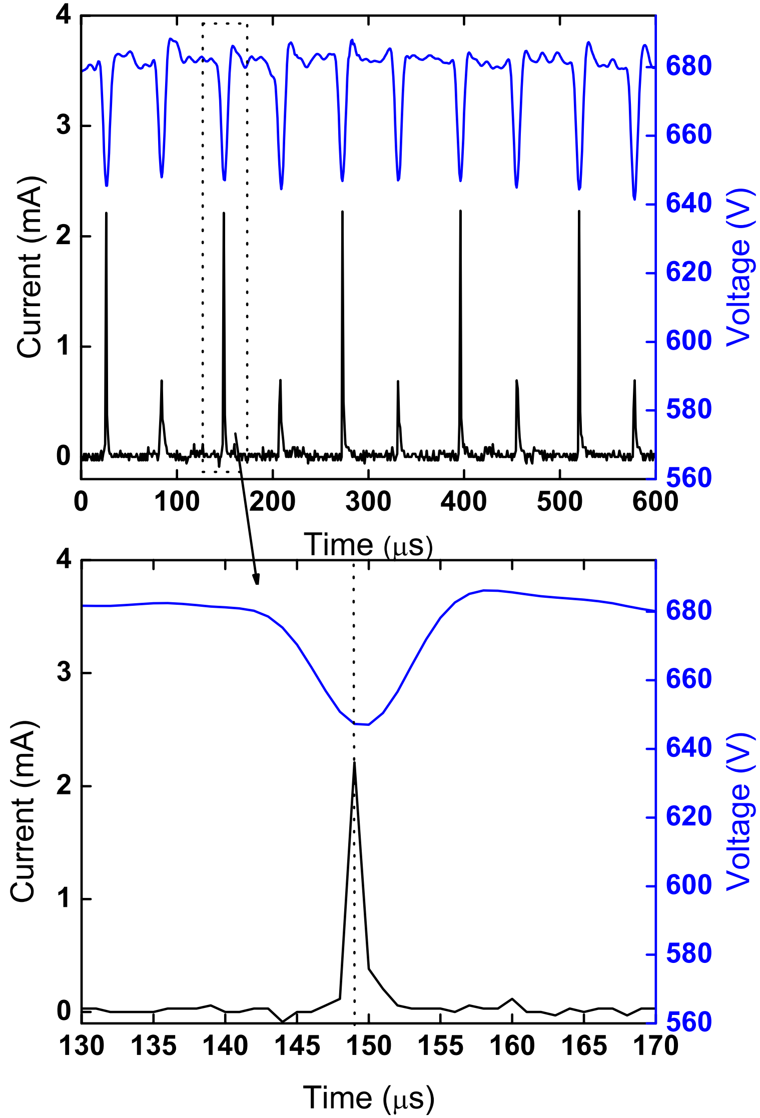

- Due to the reactive nature of the semiconductor, the left and the right side of the current oscillations are NOT symmetric.
- Current rises almost instantly in 1 μs and decays in 3 μs.
- As current rises, the voltage drops. As voltage drops and passes a certain critical value, the current begins to decay. This in return, give a rise to the voltage again sustaining the glow.
- The current response is faster compared to that of the voltage.
  - Presented as an oral talk at ICOPS, 2017 meeting, NJ, USA.

Cross Power Spectral Analysis

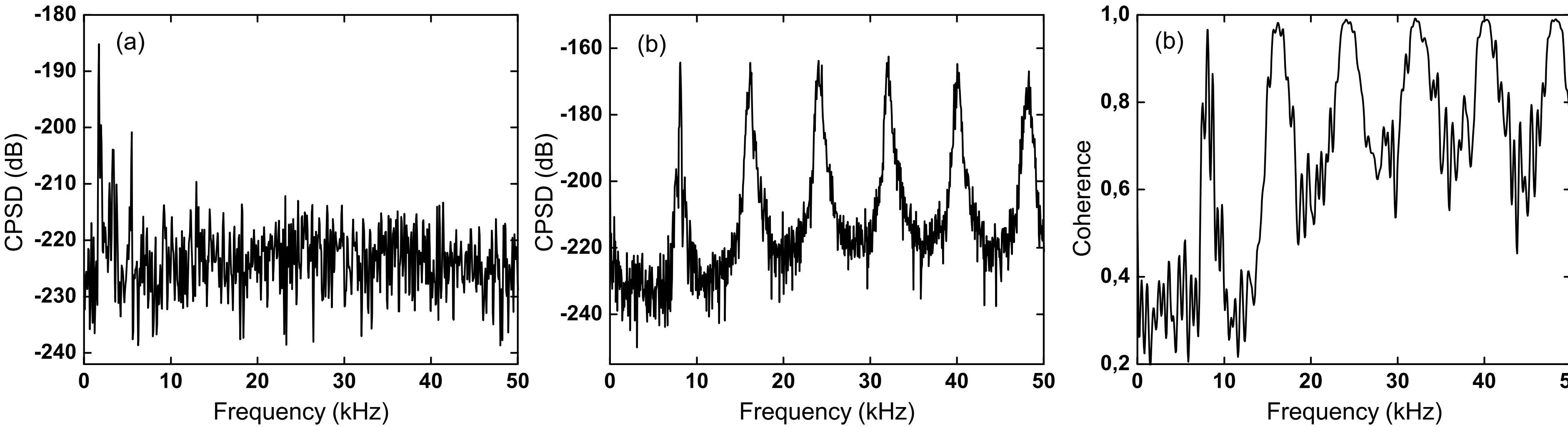

- In (a) $V_{DC} = 500V$: only one frequency and its weak harmonic are observed (f=1.7 kHz).

$$\text{CPSD}_{IV}(f_i) = < I(f_i)V^*(f_i) > = \frac{1}{L}\sum_{k=1}^{L} I_k(f_i)V^*(f_i)$$

- In (b) $V_{DC} = 580V$: As the applied voltage is increased, harmonics of the fundamental frequency changes to 8kHz and it grows stronger and becomes more coherent. Coherency is calculated using

$$\text{Coh}_{IV}(f_i) = \frac{< I(f_i)V^*(f_i) >}{\sqrt{< I(f_i)I^*(f_i) > < V(f_i)V^*(f_i) >}}$$

Cross Power Spectral Analysis and Coherence Spectrum

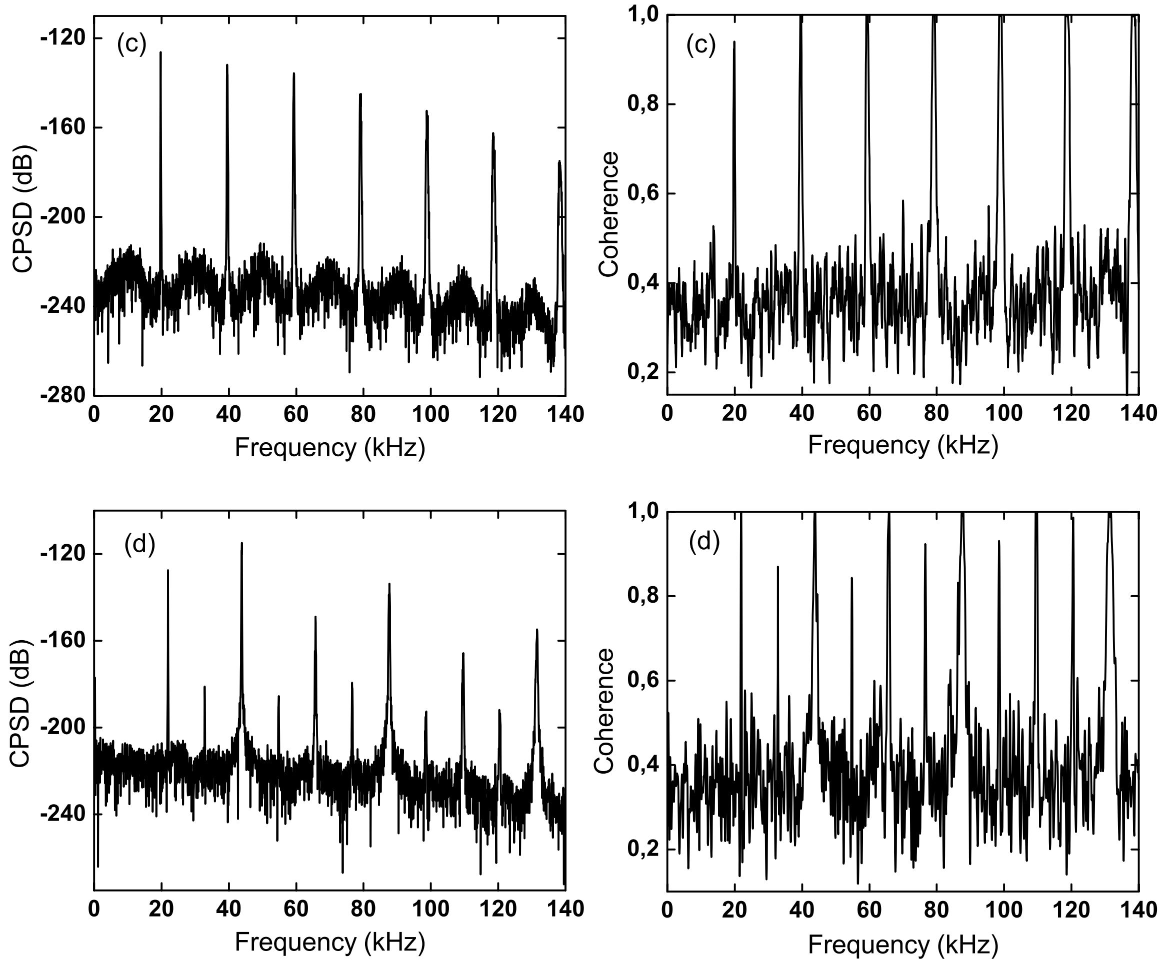

- Oscillation frequencies are about f_0=20 kHz and harmonics near $V_{DC} = 700V$.
- Subharmonic peaks observed near $f_1=f_0/2$.
- These subharmonic oscillations have broader frequency range at first.
- At (d) $V_{DC} = 980V$: As the voltage increases these subharmonics fully form into sharp coherent peaks.

Phase portraits of the system

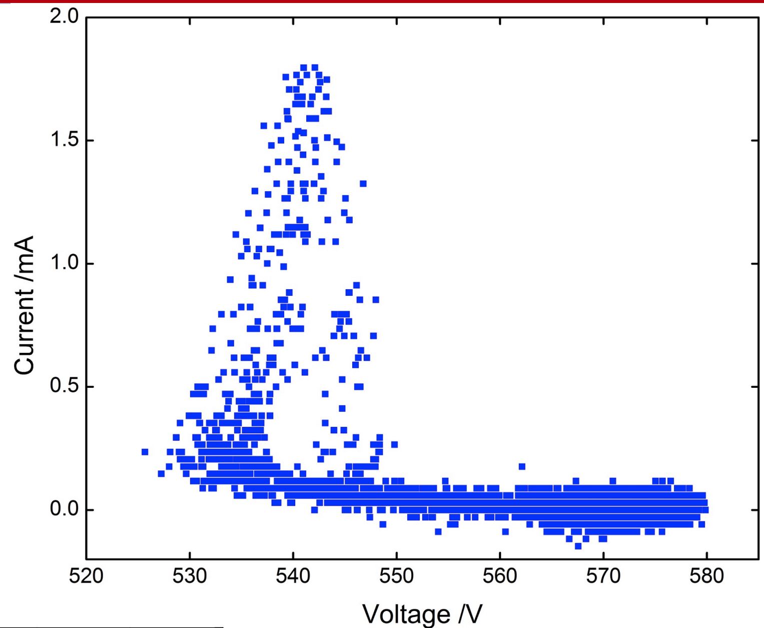

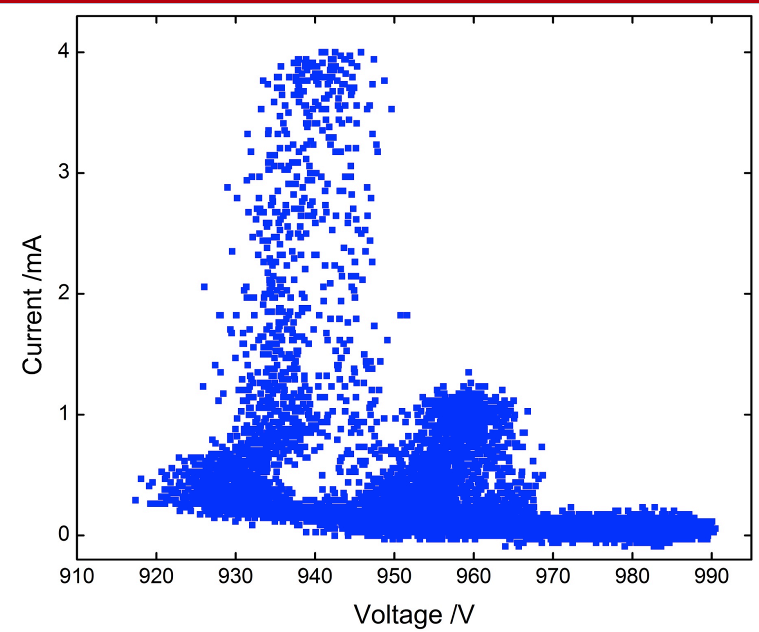

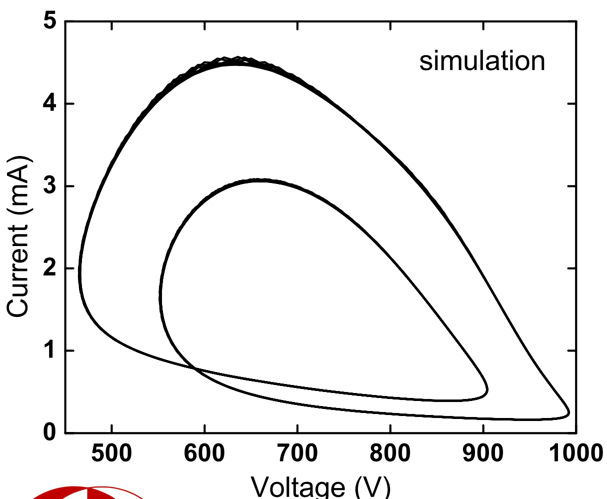

- Numerical simulation is shown on the left for 700V.
- Experimentally observed limit cycles are shown at the top:
  - a single periodic orbit(left).
  - multi-loops(right).

Limit cycle from another GaAs:Cr

- At (a) $V_{DC} = 520V$
- At (b) $V_{DC} = 800V$
- At (c) $V_{DC} = 1020V$

Published in Physics of Plasmas **24**, 053503 (2017) by D. Mansuroglu, I.Uzun-Kaymak, I. Rafatov.

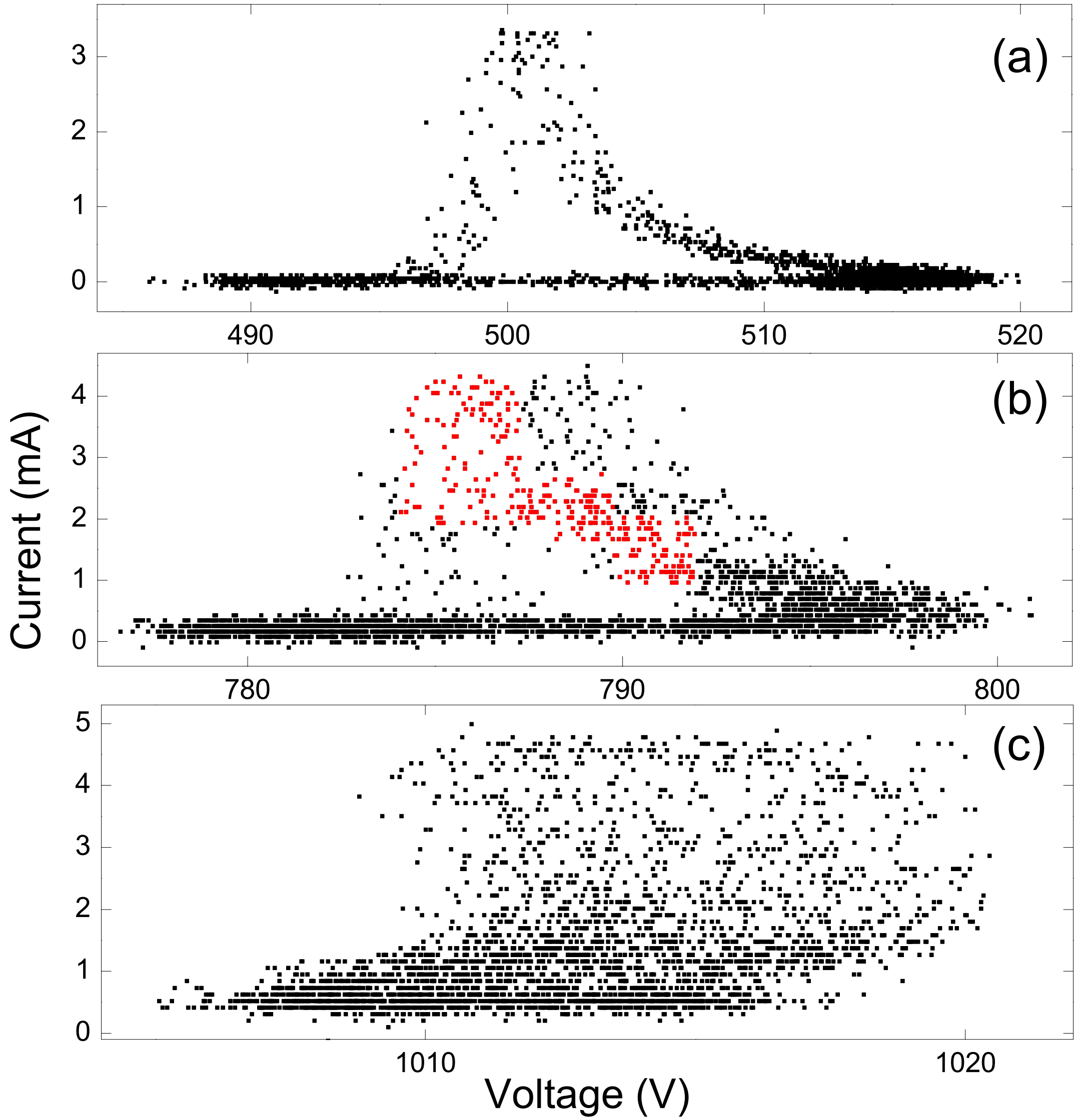

Experimental bifurcation diagram is obtained.

- **True nature of the current filaments has been shown.**
- **First time we can be able to do this measurement.**
  - Each set is 1s long.
  - Scan: Increments of 20V

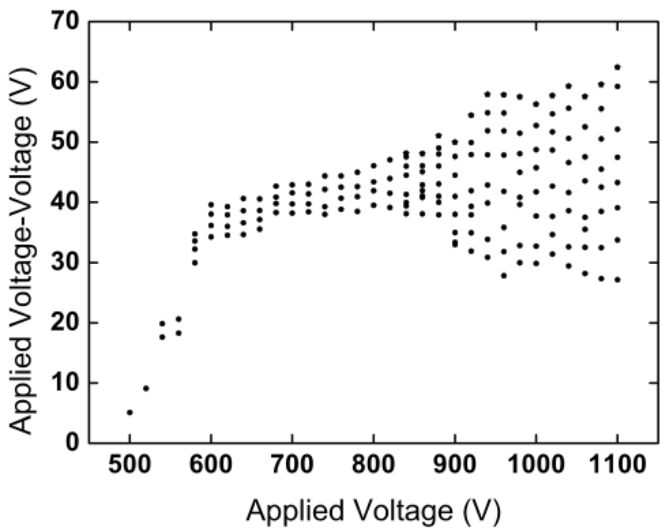

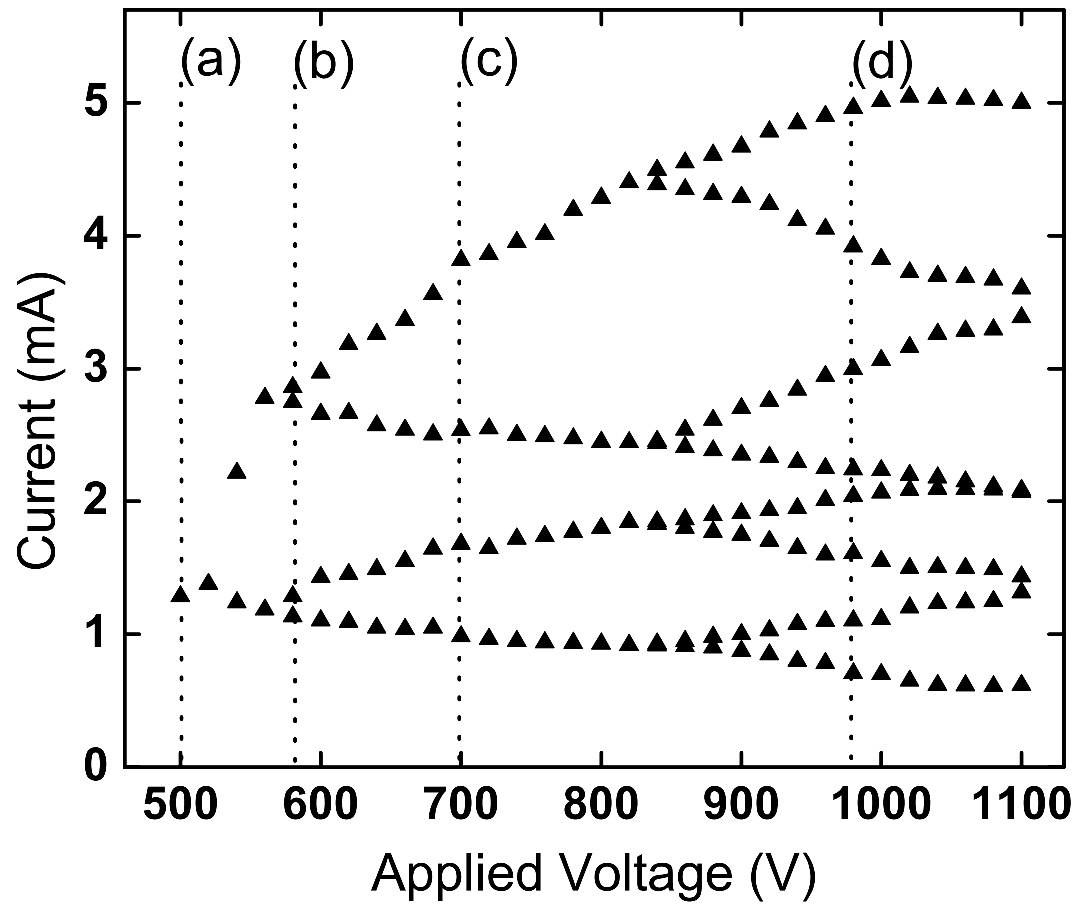

Published in Physics of Plasmas **24**, 053503 (2017) by D. Mansuroglu, I.Uzun-Kaymak, I. Rafatov.

COMSOL® Multiphysics eigenvalue solver can be used to conduct a linear stability analysis.

- Define perturbations to stationary state solutions using $f(t) = f_0 + f_1 e^{\lambda t}$
- Linearize all the equations used and convert them into an eigenvalue problem and insert equations into COMSOL®.
- Using the eigenvalue solver, solve the eigenvalue problem for a given load resistor and applied voltage.
- Vary the applied voltage using the parameter sweep mode. Look for a sign change in the solution indicating a complex conjugate. That would be the marker for the bifurcation.
- Repeat the last step by varying the conductivity constant in the numerical study.
- By plotting these markers, identify the exact location of the transition from the homogenous stationary to the homogeneous oscillatory state.

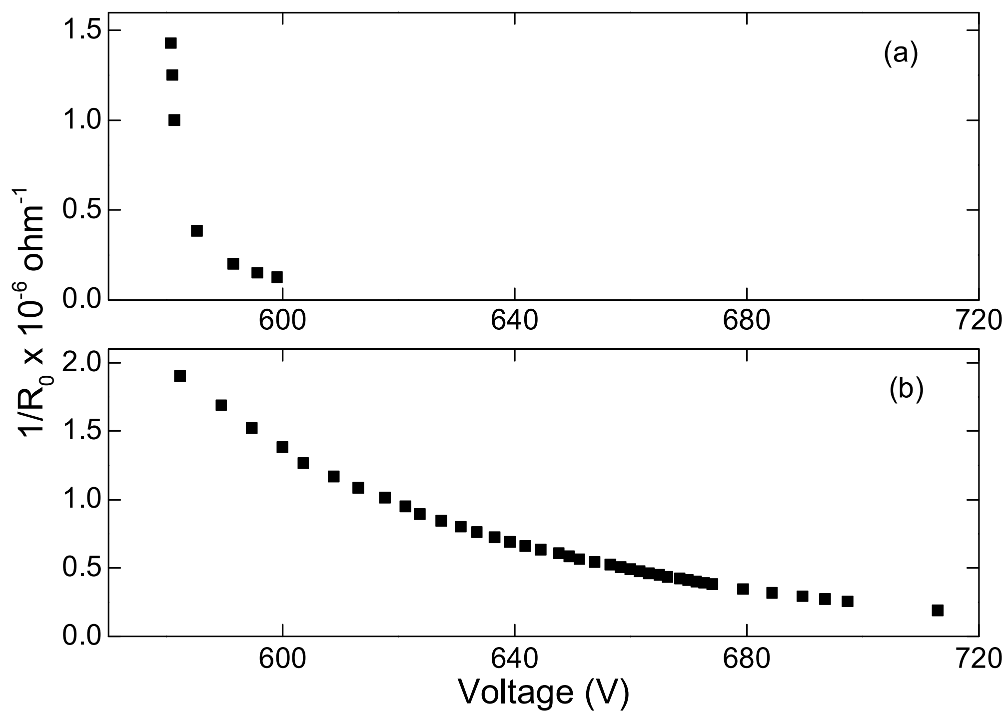

Linear stability analysis is performed experimentally(a) and results are compared with simulations(b). Published by D. Mansuroglu, I. Uzun-Kaymak, I. Rafatov in Physics of Plasmas **24**, 053503 (2017).

Summary and Acknowledgments

- Detailed analysis is carried out both numerically and experimentally for a GaAs wafer.
  - Only Hopf type bifurcations are identified as the stability configuration shifts towards periodic oscillations.
  - Simulations agree well with the experimental observations. The time-frequency evolution of the system is consistent.
  - Simulated fluctuations in COMSOL® are larger in amplitude compared to experimental observations.
  - Linear stability analysis show slight discrepancy but this is consistent with the previous studies.
- Coherency spectra tell a story about the evolution of the nonlinearity, though further studies are needed to pinpoint exact nature of the mode coupling.

This study is supported by TUBITAK Project #113C005, METU Office of Research Project # BAP-08-11-2016-044.